

Renormalised four-point coupling constant in the three-dimensional $O(N)$ model with $N \rightarrow 0$

Andrea Pelissetto

Dipartimento di Fisica and INFN – Sezione di Roma I
Università degli Studi di Roma “La Sapienza”
Piazzale Moro 2, I-00185 Roma, Italy
e-mail: Andrea.Pelissetto@roma1.infn.it

Ettore Vicari

Dipartimento di Fisica and INFN – Sezione di Pisa
Università degli Studi di Pisa
Largo Pontecorvo 2, I-56127 Pisa, Italy
e-mail: Ettore.Vicari@df.unipi.it

October 24, 2018

Abstract

We simulate self-avoiding walks on a cubic lattice and determine the second virial coefficient for walks of different lengths. This allows us to determine the critical value of the renormalized four-point coupling constant in the three-dimensional N -vector universality class for $N = 0$. We obtain $\bar{g}^* = 1.4005(5)$, where \bar{g} is normalized so that the three-dimensional field-theoretical β -function behaves as $\beta(\bar{g}) = -\bar{g} + \bar{g}^2$ for small \bar{g} . As a byproduct, we also obtain precise estimates of the interpenetration ratio Ψ^* , $\Psi^* = 0.24685(11)$, and of the exponent ν , $\nu = 0.5876(2)$.

1 Introduction

In the last thirty years there has been significant progress in the understanding of critical phenomena. The conceptual setting is now well understood and we are now in a position to check the general framework by comparing experimental and theoretical results and the different theoretical methods among themselves. The most precise experimental and theoretical results have been obtained for $O(N)$ systems in which the order parameter is an N -component vector and the symmetry breaking pattern corresponds to $O(N) \rightarrow O(N-1)$ [1]. With the increase of the precision of theoretical and experimental estimates, some small discrepancies are beginning to emerge: for instance, there is at present a discrepancy between the experimental [2,3] and the theoretical [4–6] estimates of the specific-heat exponent α for the three-dimensional XY universality class ($N = 2$); analogously, there are tiny discrepancies between the most precise field-theoretical estimates [7] of γ for three-dimensional Ising ($N = 1$) and polymer systems ($N = 0$) and those obtained by using high-temperature and Monte Carlo methods [8–11]. These differences should not be taken as an indication of the failure of the general framework; most likely, they are due to a too optimistic determination of the error bars on the results. For instance, numerical results are affected by scaling corrections which are difficult to take into account, while field-theoretical results may converge slowly due to non-analyticities of the renormalization-group functions [12–17].¹

The case $N = 0$ is a good testing ground for the different theoretical methods. Indeed, there is a well known mapping between the $N = 0$ universality class and the statistical model of self-avoiding walks (SAWs) [19]. SAWs can be very efficiently simulated by using several algorithms. In particular, in three dimensions the pivot algorithm [20–24] allows one to obtain an independent measurement of a global quantity in a time of the order of $\xi^{0.85/\nu} \sim \xi^{1.45}$ (in SAWs the correlation length ξ can be identified with the end-to-end distance) [24], to be compared with conventional algorithms for spin systems in which the autocorrelation time scales as ξ^{3+z} , where z is the dynamic critical exponent (cluster algorithms, which are at present the best ones for N -vector models, have $0 < z \lesssim 0.5$; see [25, 26] for estimates of z and additional references). Thus, for $N = 0$ one is able to probe very carefully the critical limit and get a good control of the scaling corrections that represent the main source of error in high-precision studies. Monte Carlo studies provide therefore accurate estimates of critical quantities that can be used as reference values in other theoretical approaches.

In this paper we consider the four-point renormalized coupling which is the basic ingredient in any field-theoretical calculation, computing its value at the critical point. We obtain

$$\bar{g}^* = 1.4005(5), \tag{1}$$

where \bar{g} is normalized so that the β function behaves as $\beta(\bar{g}) = -\bar{g} + \bar{g}^2 + O(\bar{g}^3)$ for small values of \bar{g} . This result should be compared with the best available estimates. Field theory gives $\bar{g}^* = 1.396(20)$ (ϵ expansion [27]) and $\bar{g}^* = 1.413(6)$ (massive zero-momentum scheme in fixed dimension $d = 3$ [7]). The ϵ -expansion result is perfectly consistent with our final estimate.

¹ Non-analyticity effects are expected to be small in three dimensions. For instance, the leading non-analytic terms appearing in the β function have the form $(g^* - g)^{1+1/\Delta}$ and $(g^* - g)^{\Delta_2/\Delta}$ [13, 15]. In three dimensions, $1 + 1/\Delta \approx \Delta_2/\Delta \approx 2$ so that non-analyticities are weak [1, 16]. This is not the case in two dimensions [17]. In the two-dimensional Ising model, a correction of the form $(g^* - g)^{8/7}$ is expected. This term is probably the reason why field-theory results [18] differ significantly from the exact ones [16, 17].

Reference	Method	$N = 0$	$N = 1$	$N = 2$	$N = 3$
[7]	FD	1.413(6)	1.411(4)	1.403(3)	1.390(4)
[27]	ϵ -exp	1.396(20)	1.408(13)	1.425(24)	1.426(9)
[6, 8, 29]	IHT		1.406(1)	1.4032(7)	1.395(7)
present work	MC	1.4005(5)			

Table 1: Estimates of the critical value of the four-point renormalized coupling \bar{g}^* in the three-dimensional N -vector model with $0 \leq N \leq 3$. We normalize \bar{g} so that the three-dimensional β function behaves as $\beta(\bar{g}) = -\bar{g} + \bar{g}^2 + O(\bar{g}^3)$. In [6, 8, 29] a different normalization is used and $g^* = 48\pi\bar{g}^*/(N + 8)$ is reported. In the second column we indicate the method used in the determination of the coupling constant. FD refers to the field-theoretical fixed-dimension zero-momentum scheme, ϵ -exp to the ϵ expansion, MC stands for Monte Carlo and IHT for the analysis of high-temperature expansions specialized to improved models (i.e. models without leading scaling corrections).

On the other hand, the fixed-dimension result differs slightly, by approximately two error bars. This is similar to what is observed for the exponent γ : the most precise fixed-dimension calculation gives [7] $\gamma = 1.1596(20)$, which is slightly larger—but fully compatible with the quoted error—than the most precise Monte Carlo estimates, $\gamma = 1.1573(2)$ [11] and $\gamma = 1.1575(6)$ [10]. A similar phenomenon occurs for $N = 1$, where the fixed-dimension estimates [7] of both \bar{g}^* and γ are slightly larger (but note that again the effect is at the level of one error bar) than the Monte Carlo results [8, 9]. The universal constant \bar{g}^* has also been computed by resumming its high-temperature expansion in the lattice N -vector model. Ref. [28] reports $\bar{g}^* = 1.388(5)$, which is not fully compatible with (1). As stressed several times [1, 15], this is probably due to scaling corrections proportional to $(\beta - \beta_c)^\Delta$, where Δ is the leading correction-to-scaling exponent ($\Delta \approx 0.5$ in the present model). Even if in principle standard resummation methods should be able to take them into account, in practice, with the series of moderate length available today, they give rise to systematic deviations that are quite difficult to estimate: as a consequence, error bars are often underestimated. This problem has been overcome by considering improved Hamiltonians characterized by the absence of leading scaling corrections [6, 8, 29], leading to accurate estimates of critical exponents and universal amplitudes for $N = 1, 2, 3$.

In Table 1 we summarize the best available estimates of \bar{g}^* for three-dimensional N -vector systems with $0 \leq N \leq 3$. Monte Carlo or high-temperature expansions computed in improved models provide the most accurate results. Field theory is in substantial agreement, although small differences appear for $N = 0$ (fixed-dimension expansion) and $N = 3$ (ϵ expansion). Other results are reported in [1].

The paper is organized as follows. In Sec. 2 we define the basic quantities that are computed in the present work. In Sec. 3 we present our numerical results. First we derive the correction-to-scaling function associated with the second virial coefficient, then we determine \bar{g}^* . Finally, in Sec. 3.3 we use our numerical data to obtain a new estimate of the exponent ν .

2 Definitions

We consider a simple cubic lattice and N -step SAWs. A SAW is a lattice walk $\{\mathbf{r}_0, \dots, \mathbf{r}_N\}$ such that \mathbf{r}_i and \mathbf{r}_{i+1} are nearest neighbors and each lattice site is visited at most once. We also introduce an effective attraction $-\mathcal{E}$ ($\mathcal{E} > 0$) between nonconnected nearest-neighbor walk sites. If $\beta \equiv -\mathcal{E}/k_B T$ is the dimensionless inverse temperature, in the scaling limit the statistical properties are independent of β as long as the system is in the good-solvent (swollen) regime. Scaling corrections instead depend on β and thus, by properly fixing β , one can reduce them significantly. Following [30], we fixed $\beta = 0.054$. The extensive Monte Carlo work of [31] indicates that for this value of β the leading scaling corrections are at least a factor-of-10 smaller than those occurring in the athermal model with $\beta = 0$.² For the simulation, we used the pivot algorithm [20–24], which is very efficient for the determination of SAW global properties. In order to estimate the zero-momentum renormalized coupling g^* , we computed the second virial coefficient for SAWs of different lengths [32]. For this purpose we used the hit-or-miss algorithm discussed in [33].

We performed a large-scale simulation, considering walks of length N varying between 100 and 64000, determining the radius of gyration and the end-to-end distance for 67 different values of N and the second virial coefficient for 369 pairs of walks of different length. Some results (those corresponding to pairs with $N_2 > N_1 \geq 8000$) are reported in Table 2. The statistics vary between 8×10^7 and 24×10^7 pivot trials for each value of N . Our runs were performed on a cluster of Intel Xeon (3.20 GHz) processors and lasted approximately 8 CPU years of a single processor.

We measured the following quantities:

- (1) The radius of gyration of a SAW of length N ,

$$R_g^2(N; \beta) \equiv \frac{1}{2(N+1)^2} \sum_{i,j} \langle (\mathbf{r}_i - \mathbf{r}_j)^2 \rangle, \quad (2)$$

where the sums go over the $N+1$ sites of the chain and \mathbf{r}_i is the corresponding position.

- (2) The end-to-end distance of a SAW of length N ,

$$R_e^2(N; \beta) \equiv \langle (\mathbf{r}_0 - \mathbf{r}_N)^2 \rangle. \quad (3)$$

- (3) The second virial coefficient for two SAWs of length N_1 and N_2 ,

$$B_2(N_1, N_2; \beta) \equiv \frac{1}{2} \sum_{\mathbf{r}} \langle 1 - e^{-\beta H(1,2)} \rangle_{\mathbf{0}, \mathbf{r}}, \quad (4)$$

where the average is over two walks of length N_1 and N_2 , the first one starting at the origin and the second at \mathbf{r} . The sum is over all lattice sites and $H(1, 2)$ is interaction energy between the two chains: $H(1, 2) = +\infty$ if the two walks intersect each other; otherwise, $H(1, 2) = -\mathcal{E} N_{nnc}$, where N_{nnc} is the number of lattice bonds $\langle \mathbf{r}_a \mathbf{r}_b \rangle$, such that \mathbf{r}_a belongs to the the first walk and \mathbf{r}_b belongs to the second walk (or vice versa).

²According to [31] scaling corrections vanish for $\beta = 0.048(7)$. Our simulations started before reference [31] was completed. For this reason we used the older estimate of [30].

λ	N_1	N_2	$V_2(N_1, N_2; \beta)$
0.1250	8000	64000	0.38972(20)
0.1406	9000	64000	0.38564(20)
0.1563	10000	64000	0.38249(20)
0.2135	10250	48000	0.37362(20)
0.2240	10750	48000	0.37236(18)
0.2292	11000	48000	0.37154(19)
0.2656	8500	32000	0.36787(19)
0.2969	9500	32000	0.36561(17)
0.4063	9750	24000	0.35963(14)
0.4432	9750	22000	0.35821(13)
0.4625	9250	20000	0.35757(8)
0.5000	12000	24000	0.35670(15)
0.5455	12000	22000	0.35536(13)
0.5469	8750	16000	0.35523(17)
0.7188	11500	16000	0.35320(15)
0.7609	8750	11500	0.35286(15)
0.8000	8000	10000	0.35278(15)
0.8125	9750	12000	0.35268(15)
0.8889	8000	9000	0.35235(14)
0.8947	8500	9500	0.35217(15)
0.9000	9000	10000	0.35248(14)
0.9167	22000	24000	0.35210(13)
0.9318	10250	11000	0.35243(12)
0.9535	10250	10750	0.35241(15)
0.9697	8000	8250	0.35214(13)
0.9773	10750	11000	0.35241(15)

Table 2: Estimates of $V_2(N_1, N_2; \beta)$ for $\beta = 0.054$. We report the Monte Carlo results such that $N_2 > N_1 \geq 8000$.

The second virial coefficient is not universal. A universal quantity is obtained by considering the following dimensionless ratio:

$$V_2(N_1, N_2; \beta) \equiv \frac{B_2(N_1, N_2; \beta)}{R_e(N_1; \beta)^{3/2} R_e(N_2; \beta)^{3/2}}. \quad (5)$$

In the scaling limit, i.e. for $N_1, N_2 \rightarrow \infty$, we have

$$R^2(N_1; \beta) = a_R(\beta) N_1^{2\nu} (1 + b_R(\beta) N_1^{-\Delta} + \dots) \quad (6)$$

$$V_2(N_1, N_2; \beta) = V^*(\lambda) + b_V(\beta) f(\lambda) (N_1 N_2)^{-\Delta/2} + \dots \quad (7)$$

where $\lambda \equiv N_1/N_2$, $f(1) = 1$ (normalization condition) and we have neglected additional subleading scaling corrections. The functions $V^*(\lambda)$ and $f(\lambda)$ as well as the exponents ν and Δ are universal. On the other hand, the amplitudes $a_R(\beta)$, $b_R(\beta)$ and $b_V(\beta)$ are model-dependent and therefore depend explicitly on β .³ The exponent ν is known quite precisely. At present the most accurate estimates are $\nu = 0.58758 \pm 0.00007$ [35], $\nu = 0.5874 \pm 0.0002$ [36] and $\nu = 0.58765 \pm 0.00020$ [11] (for an extensive list of results, see [1]). In Sec. 3.3 we confirm these results, obtaining $\nu = 0.5876 \pm 0.0002$. Also the exponent Δ has been determined quite accurately [35]: $\Delta = 0.515 \pm 0.007_{-0.000}^{+0.010}$. In Ref. [31] the second virial coefficient for walks of equal length was determined, leading to the estimate $V^*(1)(A_{ge}^*)^{-3/2} = 5.500(3)$. Using [34] $A_{ge}^* \equiv (a_{R_g}/a_{R_e})^2 = 0.15988(4)$, we obtain $V^*(1) = 0.3516(2)$.

Given $V^*(\lambda)$, the critical value of the four-point renormalized coupling constant is given by [32]

$$\bar{g}^* = \frac{6^{3/2}}{\pi} \frac{\Gamma(3\nu + 2\gamma)}{\Gamma(\gamma)^{1/2} \Gamma(\gamma + 2\nu)^{3/2}} \int_0^\infty d\lambda \lambda^{3\nu/2 + \gamma - 1} (1 + \lambda)^{-3\nu - 2\gamma} V^*(\lambda). \quad (8)$$

We use here the standard field-theoretical normalization in which the $O(N)$ β function behaves as $\beta(\bar{g}) = -\bar{g} + \bar{g}^2$ for small \bar{g} . In (8) the universal critical exponent γ appears. At present the most precise estimates are $\gamma = 1.1575(6)$ [10] and $\gamma = 1.1573(2)$ [11].

Let us note that $V_2(N_1, N_2; \beta)$ is symmetric under the interchange of N_1 and N_2 . This implies that $V^*(\lambda)$ and $f(\lambda)$ are both symmetric under the transformation $\lambda \rightarrow 1/\lambda$. In order to make this symmetry explicit we introduce a new variable

$$\mu \equiv \frac{2\lambda}{1 + \lambda^2}, \quad (9)$$

which varies in the interval $[0,1]$ and is symmetric under $\lambda \rightarrow 1/\lambda$. We take μ as fundamental variable, considering V^* and f to be functions of the variable μ . In terms of μ , integral (8) becomes

$$\bar{g}^* = \frac{6^{3/2}}{\pi} \frac{\Gamma(3\nu + 2\gamma)}{\Gamma(\gamma)^{1/2} \Gamma(\gamma + 2\nu)^{3/2}} \int_0^1 \frac{2d\mu}{\mu\sqrt{1 - \mu^2}} \left[\frac{2(1 + \mu)}{\mu} \right]^{-3\nu/2 - \gamma} V^*(\mu). \quad (10)$$

We wish now to compute the small- μ behavior of the scaling functions. For this purpose we extend a scaling argument due to de Gennes [37]. For $N_1/N_2 \rightarrow 0$, we can compute the

³The amplitude ratio $b_R(\beta)/b_V(\beta)$ is universal and therefore β independent. Estimates are reported in [34]: $b_{R_g}/b_V = -1.5(3)$, $b_{R_e}/b_V = -1.1(3)$. Also the ratio a_{R_g}/a_{R_e} is universal. Reference [34] reports $A_{ge}^* \equiv (a_{R_g}/a_{R_e})^2 = 0.15988(4)$.

second virial coefficient by dividing the longest walk (of length N_2) in N_2/N_1 blobs, which have a size of the order of the size of the shortest walk (of length N_1). The shortest SAW interacts only with a single blob, so that $B(N_1, N_2) \sim (N_2/N_1)B_{\text{bl}}(N_1)$, where $B_{\text{bl}}(N_1)$ is the second virial coefficient that takes into account the interaction between the blob and the shortest walk. Since $B_{\text{bl}}(N_1)$ depends on a single length scale, the length N_1 , by dimensional reasons we have $B_{\text{bl}}(N_1) \sim N_1^{3\nu}(1 + cN_1^{-\Delta})$. It follows

$$B(N_1, N_2) \sim N_2 N_1^{3\nu-1} (1 + cN_1^{-\Delta}), \quad (11)$$

and then

$$V_2(N_1, N_2) \sim \frac{N_2 N_1^{3\nu-1} (1 + cN_1^{-\Delta})}{N_1^{3\nu/2} (1 + d_1 N_1^{-\Delta}) N_2^{3\nu/2} (1 + d_2 N_2^{-\Delta})} \sim \lambda^{3\nu/2-1} [1 + k\lambda^{-\Delta/2} (N_1 N_2)^{-\Delta/2}]. \quad (12)$$

Comparing with the expansion (7) and taking into account that, for small λ , $\lambda \approx \mu/2$, we obtain

$$V^*(\mu) \sim \mu^{3\nu/2-1}, \quad f(\mu) \sim \mu^{3\nu/2-1-\Delta/2}. \quad (13)$$

As a consequence of this result, for $\mu \rightarrow 0$ the integrand that appears in (10) behaves as $\mu^{3\nu+\gamma-2} \sim \mu^{0.92}$. Thus, the small- μ region is not crucial for a precise determination of \bar{g}^* . This is very welcome, since it is quite difficult to determine $V^*(\mu)$ precisely for μ small.

3 Numerical results

3.1 Determination of the correction-to-scaling function $f(\mu)$

In order to determine the correction-to-scaling function $f(\mu)$ [see (7)], we use the numerical data of [30, 38]. The function $V_2(N_1, N_2; \beta)$ was determined for several values of N_1, N_2 in the range $50 \leq N_1, N_2 \leq 16000$ for $\beta = 0$ and $\beta = 0.1$, though not so precisely as in the present work. Following [30] we consider

$$R(N_1, N_2) \equiv \left(\frac{N_1}{N_2}\right)^{-\Delta/2} \frac{V_2(N_1, N_2; \beta = 0) - V_2(N_1, N_2; \beta = 0.1)}{V_2(N_1, N_1; \beta = 0) - V_2(N_1, N_1; \beta = 0.1)}, \quad (14)$$

which converges to $f(\mu)$ as $N_1, N_2 \rightarrow \infty$. In Fig. 1 we show $R(N_1, N_2)$ versus μ . The data approximately fall onto a single curve. However, at a closer look, one observes that, especially for small values of μ , the data fall on two different, though close, lines. This fact can be easily understood. The function $R(N_1, N_2)$ defined in (14) is not symmetric under the interchange of N_1 and N_2 and thus, for finite values of N_1 and N_2 , there is no symmetry under $\lambda \rightarrow 1/\lambda$. This symmetry is recovered only in the scaling limit. Thus, given a value of μ , the data cluster around two different values: one corresponds to a value of λ such that $\lambda > 1$, while the second one corresponds to a value of λ such that $\lambda < 1$. These differences disappear in the scaling limit and thus they provide us an estimate of the next-to-leading scaling corrections.

It is possible to define a quantity which is symmetric under the interchange of N_1 and N_2 and converges to $f(\mu)$ in the scaling limit. We could have defined

$$R'(N_1, N_2) \equiv \frac{V_2(N_1, N_2; \beta = 0) - V_2(N_1, N_2; \beta = 0.1)}{[\Delta V_2(N_1) \Delta V_2(N_2)]^{1/2}}, \quad (15)$$

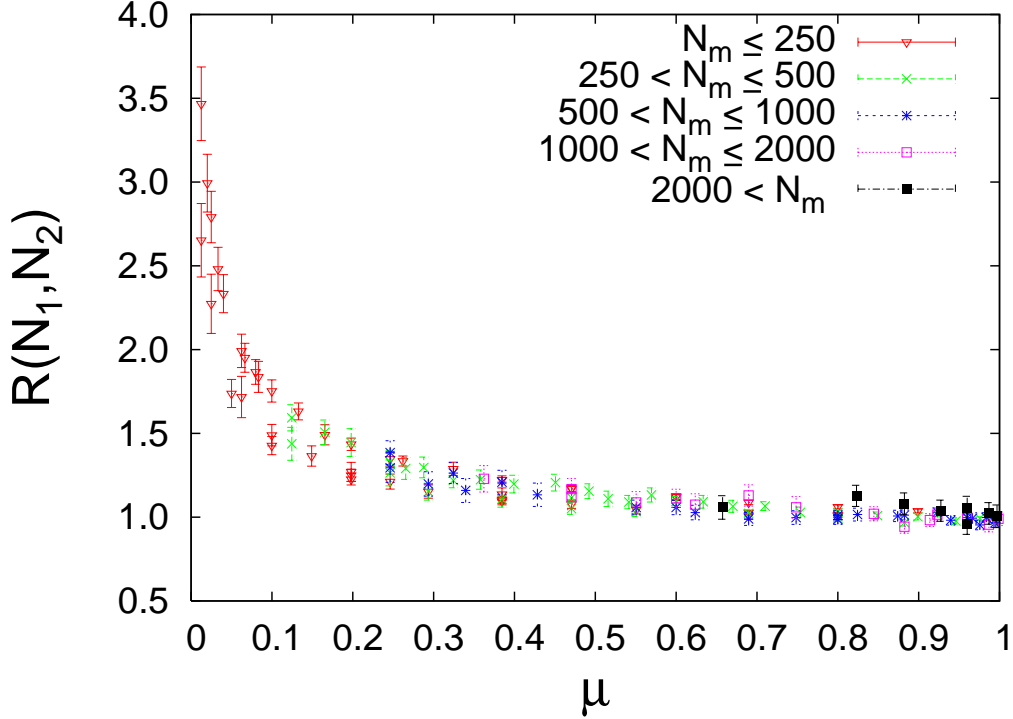


Figure 1: Plot of $R(N_1, N_2)$ as a function of $\mu \equiv 2N_1N_2/(N_1^2 + N_2^2)$, for $\Delta = 0.515$. We use different symbols according to the value of $N_m = \min(N_1, N_2)$.

where $\Delta V_2(N) \equiv V_2(N, N; \beta = 0) - V_2(N, N; \beta = 0.1)$. We could not use this definition since estimates of $\Delta V_2(N)$ are available only for a few values of N (those computed in [30]), and thus $R(N_1, N_2)$ can be determined only for 16 pairs of walks.

Since the function $f(\mu)$ behaves as $\mu^{3\nu/2-1-\Delta/2}$ as $\mu \rightarrow 0$ [equation (13)], we write

$$f(\mu) = \mu^{3\nu/2-1-\Delta/2} h(\mu), \quad (16)$$

where $h(\mu)$ satisfies $h(0) \neq 0$ and the normalization condition $h(1) = 1$. In order to estimate $h(\mu)$ we consider

$$S(N_1, N_2) \equiv R(N_1, N_2) \left(\frac{2N_1N_2}{N_1^2 + N_2^2} \right)^{-3\nu/2+1+\Delta/2}, \quad (17)$$

which converges to $h(\mu)$ in the scaling limit. The function $S(N_1, N_2)$ is reported in Fig. 2. As before, note that the data do not fall onto a single curve: two branches, corresponding respectively to $\lambda > 1$ and $\lambda < 1$ are clearly visible. Their difference gives us a rough estimate of the next-to-leading corrections. The two branches of the function $S(N_1, N_2)$ are quite smooth in μ and thus good fits are obtained by taking polynomial interpolations. Therefore, we fit the numerical data to

$$S(N_1, N_2) = 1 + \sum_{k=1}^n a_k (\mu - 1)^k, \quad (18)$$

which automatically guarantees $S(N, N) = 1$. In order to take into account the scaling corrections that show up in the presence of two different branches, we perform two fits: in

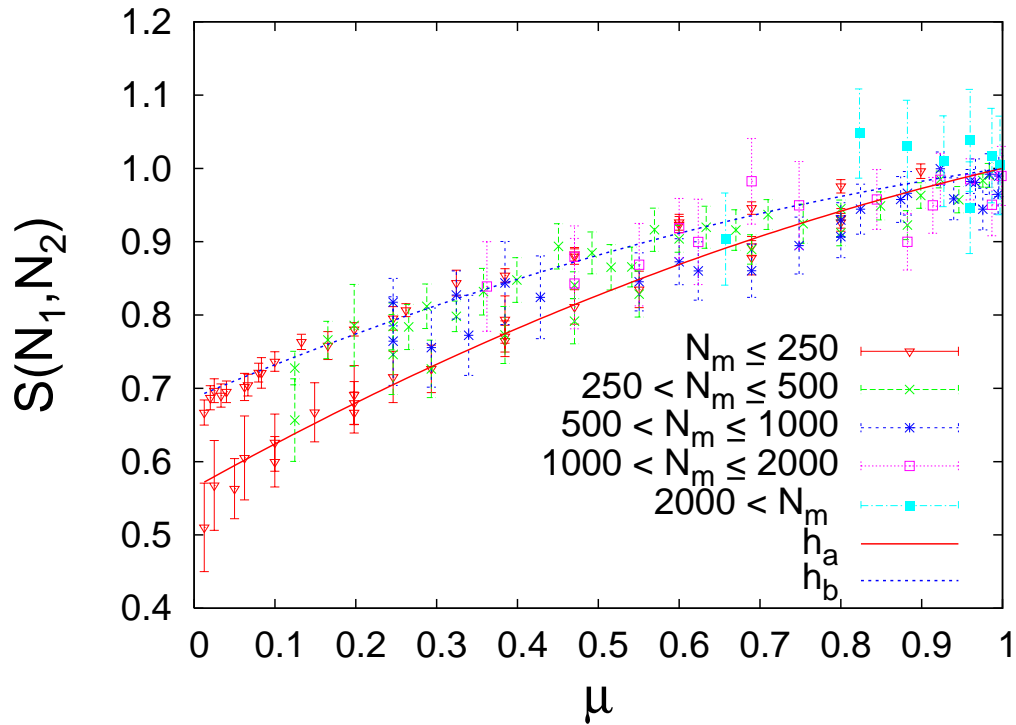


Figure 2: Plot of $S(N_1, N_2)$ as a function of $\mu \equiv 2N_1N_2/(N_1^2 + N_2^2)$, for $\Delta = 0.515$ and $\nu = 0.58758$. We use different symbols according to the value of $N_m = \min(N_1, N_2)$. We also report the functions $h_a(\mu)$ and $h_b(\mu)$ discussed in the text, see (19).

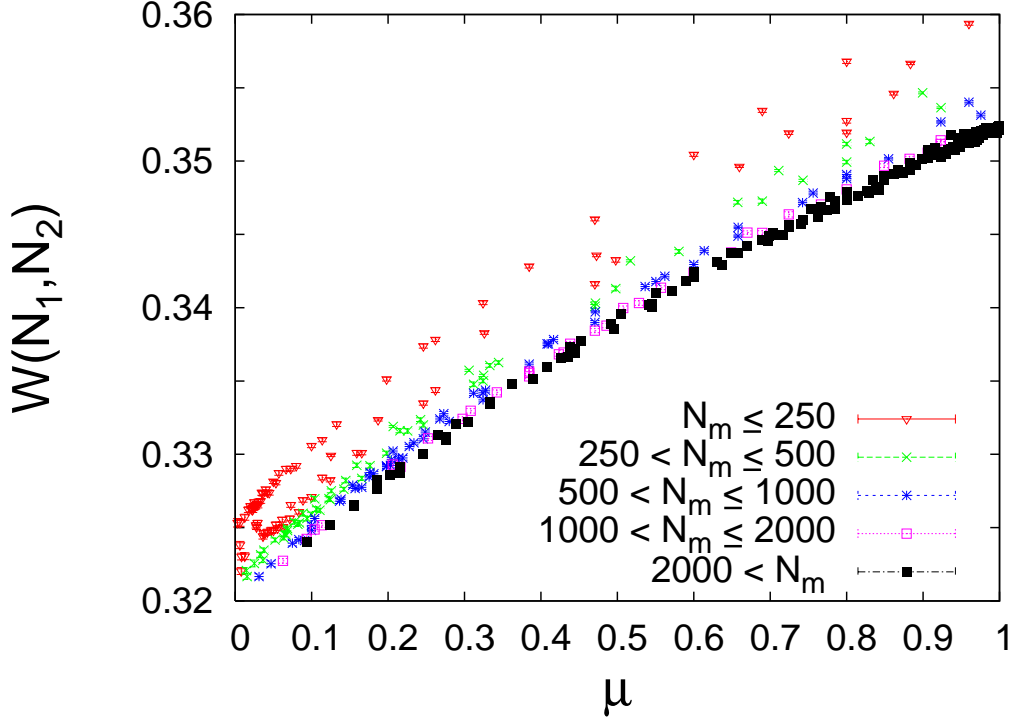


Figure 3: Plot of $W(N_1, N_2; \beta)$ for $\beta = 0.054$ as a function of $\mu \equiv 2N_1N_2/(N_1^2 + N_2^2)$ for $\nu = 0.58758$. We use different symbols according to the value of $N_m = \min(N_1, N_2)$.

the first one [fit (a)] we use all data for $\mu \geq 0.7$ and the data with $N_1 > N_2$ for $\mu < 0.7$; in the second one [fit (b)] we use all data for $\mu \geq 0.7$ and the data with $N_1 < N_2$ for $\mu < 0.7$. In case (a) we interpolate the data that belong to the lower branch, while in case (b) we interpolate the upper-branch results. The order n of the polynomial does not play much role and we always use $n = 2$. The results of the two fits are

$$\begin{aligned} h_a(\mu) &= 1 + 0.2559953(\mu - 1) - 0.179692(\mu - 1)^2, \\ h_b(\mu) &= 1 + 0.1604295(\mu - 1) - 0.152394(\mu - 1)^2. \end{aligned} \quad (19)$$

The corresponding curves are reported in Fig. 2. In the following section we use

$$h(\mu) = \frac{1}{2}[h_a(\mu) + h_b(\mu)] = 1 + 0.208212(\mu - 1) - 0.166043(\mu - 1)^2 \quad (20)$$

as our estimate of $h(\mu)$ and take $|h - h_a|$ and $|h - h_b|$ as estimates of the error on $h(\mu)$.

3.2 Estimate of g^*

We now estimate the universal function $V^*(\mu)$. Taking into account the asymptotic behavior (13), we define a new function

$$W(\mu) \equiv \mu^{1-3\nu/2}V^*(\mu), \quad (21)$$

which is such that $W(0) \neq 0$. In order to estimate $W(\mu)$ we consider

$$W(N_1, N_2; \beta) = V_2(N_1, N_2; \beta) \left(\frac{2N_1N_2}{N_1^2 + N_2^2} \right)^{-3\nu/2+1}. \quad (22)$$

For $N_1, N_2 \rightarrow \infty$ it behaves as [see (7)]

$$W(\mu) + b_V(\beta)h(\mu)\mu^{-\Delta/2}(N_1N_2)^{-\Delta/2}. \quad (23)$$

The function $W(N_1, N_2; \beta)$ is reported in Fig. 3. It shows a small dependence on μ , but significant scaling corrections. As before we use a polynomial parametrization for $W(\mu)$ and fit the data to

$$W(N_1, N_2; \beta) = \sum_{k=0}^n a_k(\mu - 1)^k + a_{n+1}h(\mu)\mu^{-\Delta/2}(N_1N_2)^{-\Delta/2}, \quad (24)$$

where we use the function $h(\mu)$ reported in (20), and a_0, \dots, a_{n+1} are fit parameters. Once $W(\mu) = \sum_{k=0}^n a_k(\mu - 1)^k$ has been determined, we can compute $V^*(\mu)$ and finally \bar{g}^* using (10). There are several sources of error on the result:

- i) Statistical errors due to the uncertainty on $V_2(N_1, N_2; \beta)$. They are computed by means of an auxiliary Monte Carlo procedure. The input data are varied randomly within error bars (at each Monte Carlo step all estimates $V_2(N_1, N_2)$ are replaced by $V_2(N_1, N_2) + r(N_1, N_2)\sigma_V(N_1, N_2)$, where $\sigma_V(N_1, N_2)$ is the error on $V_2(N_1, N_2)$ and $r(N_1, N_2)$ is a random number extracted from a Gaussian distribution with zero mean and unit variance) and \bar{g}^* is recomputed each time. The standard deviation of these estimates provides the statistical error on \bar{g}^* .
- ii) Error due to the uncertainty on $h(\mu)$. We repeat the analysis with the two functions reported in (19). The difference with the result obtained by using $h(\mu)$ gives the error.
- iii) Error due to the uncertainty of the exponents. We consider the best estimates $\nu = 0.58758(7)$, $\Delta = 0.515(17)$, and $\gamma = 1.1573(2)$, and determine how \bar{g}^* varies as the exponents change by one error bar.
- iv) Error due to the additional scaling corrections. In (7) we have only written the leading scaling correction. There are however other correction terms that vanish faster and that may be relevant at the values of N we are considering. For this purpose we have repeated the analysis several times, each time considering only data satisfying $N_1, N_2 \geq N_{\min}$, for several values of N_{\min} .

In Table 3 we give estimates of \bar{g}^* for different values of N_{\min} . We use a third-order interpolation, i.e. we set $n = 3$ in (24). Similar results are obtained for $n = 2$: for $N_{\min} \lesssim 2000$ the estimates obtained by taking $n = 2$ and $n = 3$ differ by less than $\frac{1}{3}$ of the error bar; for $N_{\min} \gtrsim 2000$ differences are larger but never exceed one error bar. The error we report is the sum of the errors of type (i), (ii) and (iii). Errors of type (ii) are always small and account for less than 5% of the total error: the somewhat large uncertainty on the function $h(\mu)$ does not have much influence on the final result. For $N_{\min} \lesssim 1000$ most of the

N_{\min}	\bar{g}^*	$V^*(1)$
100	1.3983(5)	0.35108(16)
200	1.3990(5)	0.35120(14)
400	1.3997(4)	0.35134(11)
800	1.4003(4)	0.35147(10)
1000	1.4004(4)	0.35151(10)
1500	1.4005(4)	0.35153(10)
2000	1.4004(5)	0.35150(10)
3000	1.4005(5)	0.35149(12)
5000	1.4007(7)	0.35154(19)

Table 3: Estimates of \bar{g}^* and of $V^*(1)$ for different values of N_{\min} . A third-order interpolation ($n = 3$) is used in (24).

error is due to the error on the exponent Δ , while in the opposite case the statistical error (i) dominates. As a check of our results we also report $V^*(1)$. With the parametrization (24) we have simply $V^*(1) = a_0$. The results are perfectly consistent with the estimate $V^*(1) = 0.3516(2)$ reported in Sec. 2, obtained by using the numerical results of [31, 34].

The results reported in Table 3 show a tiny dependence on N_{\min} . For $N_{\min} \geq 800$ the results are approximately constant within error bars. We take our final estimates at $N_{\min} = 3000$:

$$\bar{g}^* = 1.4005(5), \tag{25}$$

$$V^*(1) = 0.35149(12). \tag{26}$$

Estimate (25) should be compared with previous results: $\bar{g}^* = 1.396(20)$ obtained by using the ϵ expansion [27]; $\bar{g}^* = 1.413(6)$ obtained by using the massive zero-momentum scheme in three dimensions [7]; $\bar{g}^* = 1.388(5)$ obtained by resumming its high-temperature expansion [28]. Note that both the fixed-dimension estimate and the high-temperature result are not fully consistent with our results. In the case of the field-theoretical results this is probably due to the slow convergence of the perturbative expansions, a phenomenon that may be related to the non-analyticities of the renormalization-group functions at the fixed point. In the case of the high-temperature result this is probably due to the scaling corrections: resummations are not fully able to cope with the non-analyticities present at the critical point.

Our precise estimate of \bar{g}^* can also be used as input in field-theory determinations of the critical exponents γ and ν . We consider the massive zero-momentum scheme [7] in fixed dimension, in which critical quantities are obtained by evaluating the corresponding renormalization-group functions at \bar{g}^* . Instead of using the six-loop estimate $\bar{g}^* = 1.413(6)$, we evaluate the seven-loop resummed renormalization-group functions associated with γ and ν [7, 39, 40] at the Monte Carlo estimate $\bar{g}^* = 1.4005(5)$. This can be easily achieved by using some intermediate results reported in [7]. We obtain

$$\gamma = 1.1583(15), \quad \nu = 0.5873(7), \tag{27}$$

N_{\min}	$\nu(R_e^2)$	$\nu(R_g^2)$
100	0.58768(9)	0.58754(10)
200	0.58773(14)	0.58755(14)
300	0.58761(18)	0.58754(17)
400	0.58756(19)	0.58751(19)
500	0.58761(23)	0.58753(23)
600	0.58750(25)	0.58743(24)
800	0.58764(33)	0.58768(31)
1000	0.58740(36)	0.58741(34)

Table 4: Estimates of ν obtained from the analysis of R_e^2 and R_g^2 as a function of N_{\min} , the length of the shortest walk considered in the fit.

which are slightly lower than the estimates of [7], $\gamma = 1.1596(20)$ and $\nu = 0.5882(11)$, and in better agreement with the best Monte Carlo estimates $\gamma = 1.1573(2)$ and $\nu = 0.58758(7)$ mentioned above.⁴

The estimate (26) of $V^*(1)$ allows us to obtain a new estimate of the interpenetration ratio:

$$\Psi^* \equiv 2(4\pi)^{-3/2}(A_{ge}^*)^{-3/2}V^*(1) = 0.24685(11), \quad (28)$$

where we used $A_{ge}^* = 0.15988(4)$ [34]. It is consistent with the result reported in [31]: $\Psi^* = 0.24693(13)$.

3.3 Estimate of the exponent ν

As a byproduct of our simulations we obtained estimates of R_g^2 and R_e^2 up to $N = 64000$. They allow us to obtain a new estimate of the exponent ν . It is crucial to take into account the scaling corrections and thus we have performed fits of the form

$$\ln R^2 = a + 2\nu \ln N + bN^{-\Delta} + cN^{-\Delta_2}, \quad (29)$$

as we did in [31,34] for the virial coefficients, taking $\Delta = 0.515(17)$ [35] and $\Delta_2 = 1.0(1)$. The last term in (29) is an effective correction that takes into account several terms: nonanalytic corrections proportional to $N^{-2\Delta}$ and $N^{-\Delta_2}$ (Δ_2 is the next-to-leading correction-to-scaling exponent, $\Delta_2 = 0.98(6)$ [41]) and analytic terms behaving as $1/N$. As before, we repeat the fit several times, each time including data corresponding to walks such that $N \geq N_{\min}$. The results are reported in Table 4. The estimates obtained from the fits of R_g^2 are very stable—they essentially do not change for $100 \leq L_{\min} \leq 500$. Those obtained from the fits of R_e^2 show a slight downward trend but are perfectly compatible. As final estimate we take

$$\nu = 0.5876(2), \quad (30)$$

⁴One may repeat this calculation for other values of N . For example, in the Ising case ($N = 1$), using the most precise estimate $\bar{g}^* = 1.406(1)$, see Table 1, one obtains $\gamma = 1.2387(8)$ and $\nu = 0.6299(10)$, which should be compared with the field-theoretical estimates [7] $\gamma = 1.2396(13)$ and $\nu = 0.6304(13)$ (obtained by using the six-loop result $\bar{g}^* = 1.411(4)$), and the lattice results [9, 29] $\gamma = 1.2373(2)$ and $\nu = 0.63012(16)$.

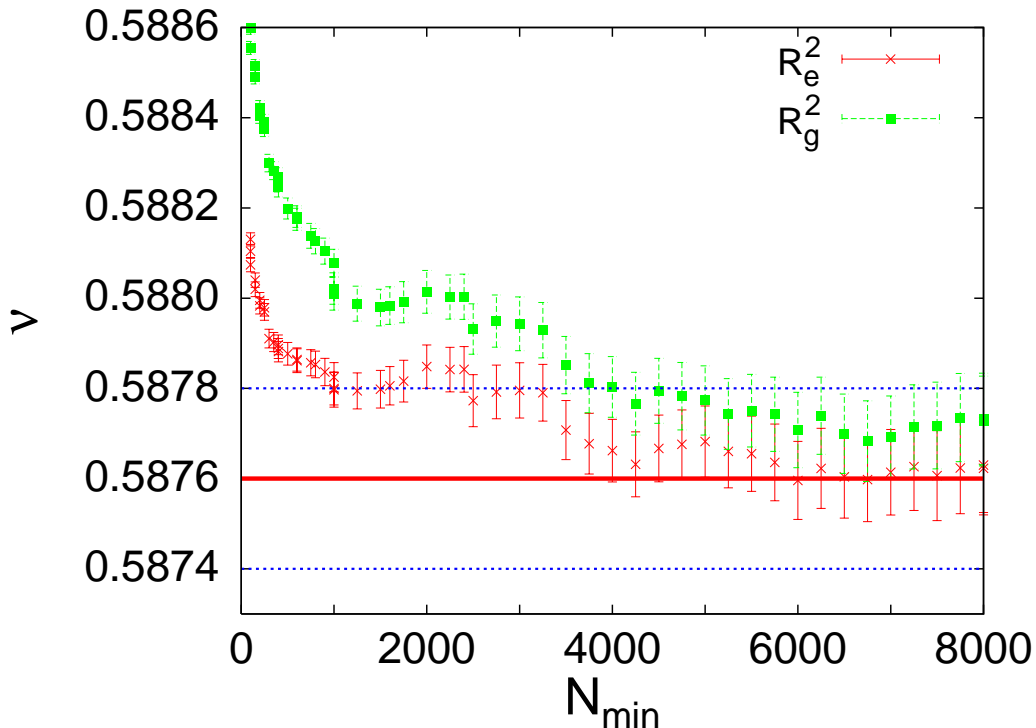


Figure 4: Estimates of ν obtained by fitting R_g^2 and R_e^2 to $\ln R^2 = a + 2\nu \ln N$, as a function of N_{\min} , the length of the shortest walk considered in the fit. The thick horizontal line corresponds to our central estimate (30), while the thin dotted lines give the error.

which is compatible with all results reported in Table 4. The estimate (30) is in good agreement with the previous ones reported in the literature [11, 35, 36] and mentioned in Section 2.

Note that inclusion of the scaling corrections in the fit is crucial. In Fig. 4 we report the estimates of ν obtained by using a fit without scaling corrections, $\ln R^2 = a + 2\nu \ln N$. The results show a clear downward trend, depend on the quantity at hand, and are apparently constant within error bars only for $N_{\min} \gtrsim 6000$. In this range they are in perfect agreement with the estimate (30).

Acknowledgements

The numerical results presented here have been obtained on the Theory cluster at CNAF (INFN) in Bologna.

References

- [1] Pelissetto A and Vicari E 2002 *Phys. Rept.* **368** 549.
- [2] Lipa J A, Swanson D R, Nissen J, Chui T C P and Israelson U E 1996 *Phys. Rev. Lett.* **76** 944

- [3] Lipa J A, Nissen J, Stricker D A, Swanson D R and Chui T C P 2003 *Phys. Rev. B* **68** 174518
- [4] Campostrini M, Hasenbusch M, Pelissetto A, Rossi P and Vicari E 2001 *Phys. Rev. B* **63** 214503
- [5] Burovski E, Machta J, Prokof'ev N and Svistunov B 2006 *Phys. Rev. B* **74** 132502
- [6] Campostrini M, Hasenbusch M, Pelissetto A and Vicari E 2006 *Phys. Rev. B* **74** 144506
- [7] Guida R and Zinn-Justin J 1998 *J. Phys. A: Math. Gen.* **31** 8103
- [8] Campostrini M, Pelissetto A, Rossi P and Vicari E 2002 *Phys. Rev. E* **65** 066127
- [9] Deng Y and Blöte H W J 2003 *Phys. Rev. E* **68** 036125
- [10] Caracciolo S, Causo M S and Pelissetto A 1998 *Phys. Rev. E* **57** R1215
- [11] Hsu H-P, Nadler W and Grassberger P 2004 *Macromolecules* **37** 4658
- [12] Nickel B G 1982 in *Phase Transitions*, edited by Lévy M, Le Guillou J C and Zinn-Justin J (New York and London: Plenum Press)
- [13] Nickel B G 1991 *Physica A* **177** 189
- [14] Sokal A D 1994 *Europhys. Lett.* **27** 661
- [15] Pelissetto A and Vicari E 1998 *Nucl. Phys. B* **519** 626
- [16] Caselle M, Pelissetto A and Vicari E 2001 in *Fluctuating Paths and Fields*, edited by Janke W, Pelster A, Schmidt H-J and Bachmann M (Singapore: World Scientific) [hep-lat/0010228]
- [17] Calabrese P, Caselle M, Celi A, Pelissetto A and Vicari E 2000 *J. Phys. A: Math. Gen.* **33** 8155
- [18] Orlov E V and Sokolov A I 2000 *Fiz. Tverd. Tela* **42** 2087; (English translation) Orlov E V and Sokolov A I 2000 *Phys. Solid State* **42** 2151
- [19] de Gennes P G 1979 *Scaling Concepts in Polymer Physics* (Ithaca, NY: Cornell University Press)
- [20] Lal M 1969 *Molec. Phys.* **17** 57
- [21] MacDonald B, Jan N, Hunter D L and Steinitz M O 1985 *J. Phys. A: Math. Gen.* **18** 2627
- [22] Madras N and Sokal A D 1988 *J. Stat. Phys.* **50** 109
- [23] Sokal A D 1995 in *Monte Carlo and Molecular Dynamics Simulations in Polymer Science*, edited by Binder K (Oxford: Oxford Univ. Press)

- [24] Kennedy T 2002 *J. Stat. Phys.* **106** 407
- [25] Ossola G and Sokal A D 2004 *Nucl. Phys. B* **691** 259
- [26] Coddington P D and Baillie C F 1992 *Phys. Rev. Lett.* **68** 962
- [27] Pelissetto A and Vicari E 2000 *Nucl. Phys. B* **575** 579
- [28] Butera P and Comi M 1998 *Phys Rev. B* **58** 11552
- [29] Campostrini M, Hasenbusch M, Pelissetto A, Rossi P and Vicari E 2002 *Phys Rev. B* **65** 144520
- [30] Pelissetto A and Hansen J P 2005 *J. Chem. Phys.* **122** 134904
- [31] Caracciolo S, Mognetti B M and Pelissetto A 2006 *J. Chem. Phys.* **125** 094903
- [32] Muthukumar M and Nickel B G 1987 *J. Chem. Phys.* **86** 460
- [33] Li B, Madras N and Sokal A D 1995 *J. Stat. Phys.* **80** 661
- [34] Caracciolo S, Mognetti B M and Pelissetto A 2006 *J. Chem. Phys.* **125** 094904 Erratum 2007 *J. Chem. Phys.* **126**
- [35] Belohorec P and Nickel B G 1997 *Accurate universal and two-parameter model results from a Monte-Carlo renormalization group study*, Guelph University report, unpublished
- [36] Prellberg T 2001 *J. Phys. A: Math. Gen.* **34** L599
- [37] de Gennes P G 1982 talk cited in Witten T A and Prentis J J 1982 *J. Chem. Phys.* **77** 4247
- [38] Pelissetto A 2006 *Macromolecules* **39** 4184
- [39] Baker Jr G A, Nickel B G, Green M S and Meiron D I 1977 *Phys. Rev. Lett.* **36** 1351
- [40] Murray D B and Nickel B G 1991 *Revised estimates for critical exponents for the continuum n-vector model in 3 dimensions*, Guelph University report, unpublished
- [41] Newman K E and Riedel E K 1984 *Phys. Rev. B* **30** 6615